

## Stability of discrete age-structured and aggregated delay-difference population models

M. O. Bergh and W. M. Getz

Division of Biological Control, University of California, Berkeley, 1050 San Pablo Avenue, Albany, CA 94706, USA

**Abstract.** Sufficiency conditions for local stability are derived for a class of density dependent Leslie matrix models. Four of the recruitment functions in common use in fisheries management are then considered. In two of these oscillating instability can never occur (Beverton and Holt and Cushing forms). In the other two (Deriso–Schnute and Shepherd forms) undamped oscillations are possible within the region of parameter space described here. An algorithm is developed for calculating necessary and sufficient local stability conditions for a simplified form of the general age-structured model. The complete spectrum of stability states (monotonic stability; monotonic instability; oscillating-stable; oscillating-unstable) and the bifurcation periods are given for selected examples of this model. The examples cover a large portion of the parameter space of interest in resource management. It is shown that in perfectly deterministic systems which are observed with error, oscillating instabilities may be missed, and such systems could be erroneously assumed to be stable.

**Key words:** Stability — Discrete population models — Bifurcation

### 1. Introduction

The concept of autoregulated equilibria in animal population models has had considerable application in contemporary ecological research. However, elementary models previously thought to be useful for summarising, simplifying and interpreting ecological data have been shown to be capable of quite extraordinary dynamic complexity (May and Oster (1976)). The mechanics of this complexity has been explored in detail by May (1976) and others, for some selected, analytically tractable examples. Briefly, as parameter values change, equilibria of very simple single species population models may undergo an initial bifurcation from being stable to being unstable. In the non-delay discrete case, the first

bifurcation usually results in a stable two cycle. As parameter values are changed, the two cycle might bifurcate to a stable four cycle. Repeated bifurcations can be made to occur, until at some point in parameter space there are no stable periodic attractors. In this region the dynamics are termed chaotic.

Even if an equilibrium is locally stable the dynamic behaviour in the region of this equilibrium can be diverse. It is possible to classify the return paths into two categories; either damped oscillatory behaviour, or geometric, monotonic behaviour. In this paper we focus on the conditions which are necessary for oscillating instability to occur and on classifying the region of stability as either damped oscillatory or monotonic geometric decay.

Papers by May et al. (1974), May (1976), May and Oster (1976), Levin and May (1976), Clark (1976), Goh (1977), Botsford and Wickam (1978), Levin and Goodyear (1980), and Fisher and Goh (1984) deal with mathematical definitions of the conditions required for oscillatory instability. In Levin and May (1976), the local stability region of parameter space is classified according to whether behaviour is oscillatory or monotonic. The above papers cover a wide spectrum of population models. The purpose of this paper is to develop the local stability analysis for discrete populations with age-structure. Thus, in contrast to researchers concerned with chaos, we do not venture beyond the threshold into the region of instability. From our experience in analysing and computing the dynamics of these models we believe that the conditions at the bifurcation threshold are informative above what happens in the unstable region. Bifurcation periods are thus presented as plausible first estimates of the fully non-linear periods of oscillation.

Although there is a substantial review component in this paper, new results are reported. These are the delineation of sufficient stability conditions for a density dependent form of Leslie's (1945) model for four different recruitment functions, and the necessary conditions and an algorithm for determining the stability state and bifurcation periods of Deriso's (1978) model with arbitrary delay. In the case of Deriso's model the stability conditions are both necessary and sufficient; numerical results are given for a wide range of parameter values.

Our analysis of Deriso's model subsumes the earlier work on special forms by Clark (1976) and Levin and May (1976). Whereas Clark's analysis considers the effect of adult survivorship and time delays on stability, the analysis of Deriso's model clarifies the consequences of adult growth rate when fecundity is proportional to body size, as occurs for several fish populations.

Oscillations in population abundance are important in the management of marine and many other resource systems. When these oscillations are periodic then special management regulations may be needed. To determine whether sustained oscillations occur in a population, the stability properties of equilibria are assessed by evaluating the slope of the recruitment function at these equilibria. If state variables such as recruitment levels and adult population size are measured with error, then estimates of the slope of the recruitment function are likely to be biased. We present an analysis, using results from Walters and Ludwig (1981), which indicate that systems which are indeed dynamically unstable may frequently be erroneously classified as deterministically stable. This problem deserves cognizance in the field of resource management.

We begin by describing the most general form of the demographic models treated here.

## 2. A discrete demographic model

The most general model considered here is a discrete age-structured population model in which non-linearities only occur in the first year survivorship. This model has been widely used in fisheries management (Getz (1980, 1988), Hightower and Grossman (1985), Levin and Goodyear (1981), Reed (1980)) as well as other population harvesting problems (Fowler and Smith (1973), Getz and Haight (in press)).

We define the population vector  $\bar{N}(t+1)$ , where

$$\bar{N}(t) = \begin{pmatrix} N_1(t) \\ N_2(t) \\ \vdots \\ N_n(t) \end{pmatrix}. \quad (1)$$

The entries  $N_i(t+1)$  represent the number of individuals at the beginning of year  $t$  which are  $i$  years old. Let the population matrix be  $A$ , so that

$$\bar{N}(t+1) = A\bar{N}(t). \quad (2)$$

We assume that the number of fertilized zygotes produced at the beginning of year  $t$ ,  $N_0(t)$ , is a weighted sum of the number of individuals aged 1 year and older, i.e.

$$N_0(t) = \sum_{i=1}^n b_i N_i(t), \quad (3)$$

where  $b_i$  are the number of zygotes produced per adult individual, assuming a monoecious population (or female zygotes produced per female if we only model the female portion of the population). The zygotes in Eq. (3) are assumed to experience both density-dependent and density-independent mortality in their first year of life. We let the first year survivorship factor be a nonlinear function,  $\phi(N_0(t))$ , where  $0 < \phi(N_0(t)) < 1$ ;  $\phi(0) = 1$ , and  $d\phi(x)/dx < 0$  for  $x > 0$ . The first year density-independent survivorship factor is  $s_0$ . Total survivorship is a product of density-dependent and density-independent survivorship, so that

$$N_1(t+1) = s_0 \phi(N_0(t)) N_0(t) \quad (4)$$

and for ages other than the first year, survivorship is density-independent. That is

$$N_{i+1}(t+1) = s_i N_i(t) \quad (5)$$

where  $s_i$  is the density-independent survivorship factor for age class  $i$ .  $A$  now

has the explicit form

$$A = \begin{bmatrix} b_1 s_0 \phi(N_0(t)) & b_2 s_0 \phi(N_0(t)) & \cdots & b_{n-1} s_0 \phi(N_0(t)) & b_n s_0 \phi(N_0(t)) \\ s_1 & & & & \\ \vdots & s_2 & \vdots & \vdots & \vdots \\ & & & s_{n-1} & 0 \end{bmatrix}. \tag{6}$$

Define  $l_i = s_0 s_1 s_2 \cdots s_{i-1}$ , which implies that  $l_1 = s_0$ . From (5) it follows that

$$N_i(t) = \frac{l_i}{l_1} N_1(t - i + 1) \tag{7}$$

Substituting  $\sum_{i=1}^n b_i N_i(t)$  for  $N_0(t)$  in (4) gives

$$N_1(t + 1) = s_0 \sum_{i=1}^n b_i N_i(t) \phi\left(\sum_{i=1}^n b_i N_i(t)\right). \tag{8}$$

Then substituting  $(l_i/l_1)N_1(t - i + 1)$  for  $N_i(t)$  in (8) gives

$$\begin{aligned} N_1(t + 1) &= s_0 \sum_{i=1}^n b_i \frac{l_i}{l_1} N_1(t - i + 1) \phi\left(\sum_{i=1}^n b_i \frac{l_i}{l_1} N_1(t - i + 1)\right) \\ &= \sum_{i=1}^n b_i l_i N_1(t - i + 1) \phi\left(\sum_{i=1}^n b_i \frac{l_i}{l_1} N_1(t - i + 1)\right). \end{aligned} \tag{9}$$

The dynamics of  $N_1(t)$  are completely described by the maternity schedules,  $b_i l_i$ , the value of  $l_1$  and the function  $\phi$ . Therefore, since  $b_i$  and  $s_i$  only appear as a product, high values of adult mortality and fertility could produce the same dynamics as low values of adult mortality and fertility.

For our analysis it is convenient to define the reproductive value  $R_0$ ,

$$R_0 = \sum_{i=1}^n b_i l_i.$$

We now examine the stability of models of form (9) for some special cases of  $\phi$ .

### 2.1. Stability results

Suppose  $\bar{N}^*$  is an equilibrium solution. Then it follows from Eqs. (4), (7), (8) and (9) that the equilibrium zygote level satisfies

$$N_0^* \phi(N_0^*) = N_0^* / R_0. \tag{10}$$

In the plot of  $N_0 \phi(N_0)$  versus  $N_0$  shown in Fig. 1, the line passing through the origin with slope  $1/R_0$  is termed the replacement line, since in the linear model ( $\phi(N_0) = 1$ ) it corresponds to each individual exactly replacing itself throughout its life. The equilibria for the non-linear model are the points of intersection of  $N_0 \phi(N_0)$  with the replacement line  $N_0/R_0$  (Fig. 1).

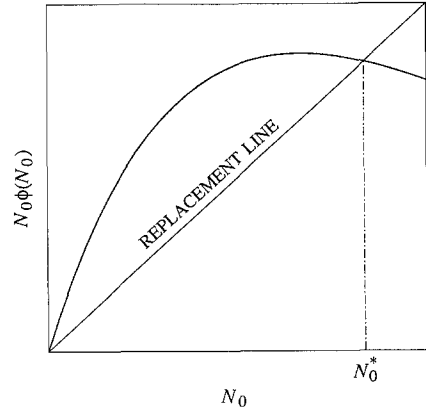


**Fig. 1.** Example of a concave stock-recruit relationship, as a plot of  $N_0\phi(N_0)$  vs.  $N_0$ , showing the replacement line and the equilibrium point

Local stability for the demographic model shown in the previous section is assured if the eigenvalues of the population matrix linearized around the equilibrium  $\bar{N}^*$  all lie within the unit circle. The characteristic polynomial for the linearized population matrix is developed in Levin and Goodyear (1980). In terms of our notation, it is

$$\frac{d}{dN_0} [N_0\phi(N_0)]|_{N_0=N_0^*} \sum_{i=1}^n \lambda^{-i} b_i l_i = 1 \tag{11}$$

i.e. the familiar Perron equation. The Perron–Frobenius theorem puts bounds on the modulus of the dominant eigenvalue, if the population matrix is non-negative; i.e. if the coefficients of  $\lambda^{-i}$  in (11) are all zero or positive, the terms  $b_i l_i$  are all positive. However,  $d[N_0\phi(N_0)]/dN_0$  could be negative at equilibrium. Therefore the Perron–Frobenius theorem is limited to cases where the slope of the recruitment function at equilibrium is positive. If the slope is positive, then the dominant eigenvalue is real and positive. The upper bound on the size of this dominant positive eigenvalue,  $\lambda$ , given by the Perron–Frobenius theorem, is (Reed (1980))

$$\lambda < \frac{d}{dN_0} [N_0\phi(N_0)]|_{N_0=N_0^*} R_0. \tag{12}$$

A matrix result due originally to Minc and Marcus (1964) and cited recently by Reed (1980) extends the Perron–Frobenius result to negative matrices, placing bounds on the modulus of the dominant eigenvalue. The dominant eigenvalue could be real or complex, and the bounds on its modulus are

$$|\lambda| < \left| \frac{d}{dN_0} [N_0\phi(N_0)]|_{N_0=N_0^*} \right| R_0. \tag{13}$$

For the modulus of the dominant eigenvalue to be less than unity, we need the condition

$$\left| \frac{d}{dN_0} [N_0\phi(N_0)]|_{N_0=N_0^*} \right| < \frac{1}{R_0} \tag{14}$$

to be satisfied, which is equivalent to

$$-\frac{1}{R_0} < \frac{d}{dN_0} [N_0\phi(N_0)]|_{N_0=N_0^*} < \frac{1}{R_0}. \tag{15}$$

These are sufficiency conditions only, since the left-hand inequality can be violated and the system may nevertheless be locally stable.

If  $N_0\phi(N_0)$  is some generally concave function of  $N_0$  which passes through the origin (see Fig. 1) then there will only be one equilibrium point. In this case it is not geometrically possible for the slope of  $N_0\phi(N_0)$  to be both positive and steeper than the slope of the replacement line at equilibrium, i.e. the right-hand inequality of condition (15) cannot be violated. This can only occur if the recruitment function becomes convex, in which case the equilibrium state is unstable. Thus for functions  $N_0\phi(N_0)$  which are both positively sloped and concave, instability is mathematically impossible.

For example, two well known recruitment functions are the Beverton and Holt (1957) and Cushing (1973) functions familiar to fisheries biologists, that is, respectively

$$N_1 = \frac{s_0 N_0}{k + N_0}, \quad k > 0 \tag{16}$$

and

$$N_1 = s_0 N_0^\mu, \quad 0 < \mu < 1. \tag{17}$$

Both these functions are concave in terms of their arguments (i.e. the second derivative is negative). Both have strictly positive derivatives for positive arguments. Thus condition (15) is never violated and instability cannot occur.

Consider next the Deriso-Schnute (Deriso (1978), Schnute (1985)), and Shepherd (1982) recruitment functions, which respectively are

$$N_1 = s_0 N_0 (1 - \gamma\beta N_0)^{1/\gamma} \tag{18}$$

and

$$N_1 = \frac{s_0 N_0}{1 + (N_0/K)^\nu}. \tag{19}$$

Special cases of the Deriso-Schnute equation are the Ricker function ( $\gamma = 0$ ), the Beverton and Holt function ( $\gamma = -1$ ), and the logistic function ( $\gamma = +1$ ). The best known special case of the Shepherd function is the Beverton and Holt function,  $\nu = 1$ , mentioned earlier. When  $\nu = 2$  the Shepherd function has a Ricker-like shape (i.e. it approaches 0 asymptotically as  $N_0$  approaches infinity — Shepherd (1982)).

The derivatives at equilibrium for the Deriso-Schnute and Shepherd forms are given below

Deriso-Schnute:

$$\frac{dN_1}{dN_0} \Big|_{N_0=N_0^*} = \frac{l_1}{R_0} \left[ 1 - \frac{1}{\gamma} [(R_0)^\gamma - 1] \right]. \tag{20}$$

Shepherd:

$$\left. \frac{dN_1}{dN_0} \right|_{N_0=N_0^*} = \frac{l_1}{R_0} \left[ 1 - \nu + \frac{\nu}{R_0} \right]. \quad (21)$$

The equilibrium values of  $N_0$  are

Deriso-Schnute:

$$N_0^* = \frac{1}{\gamma} \left[ 1 - \left[ \frac{1}{R_0} \right]^\gamma \right]. \quad (22)$$

Shepherd:

$$N_0^* = K(R_0 - 1)^{1/\nu}. \quad (23)$$

Both functions thus require that  $R_0 > 1$  for biological realism. If  $\nu$  is negative, the Shepherd recruitment function is convex; therefore we consider only  $\nu \geq 0$ . Placing the derivatives into the matrix condition for stability (15), but considering only the left-hand side, gives

Deriso-Schnute:

$$-1 < 1 - \frac{1}{\gamma} ((R_0)^\gamma - 1). \quad (24)$$

Shepherd:

$$-1 < 1 - \nu + \frac{\nu}{R_0}. \quad (25)$$

We deal first with the Deriso-Schnute form. If  $\gamma$  is positive then the sufficiency condition for stability and simultaneous biological realism becomes

$$1 < R_0 < (1 + 2\gamma)^{1/\gamma}. \quad (26)$$

There is a region of stability for all positive  $\gamma$  (since  $(1 + 2\gamma)^{1/\gamma} > 1$  for all  $\gamma > 0$ ). If  $\gamma$  is negative, then, letting  $a = -\gamma$ , stability is guaranteed if

$$1 - 2a < \frac{1}{(R_0)^a}. \quad (27)$$

This always holds if  $a > \frac{1}{2}$  (i.e.  $\gamma < -\frac{1}{2}$ ) regardless of the maternity values  $b_i l_i$ . For  $0 < a < \frac{1}{2}$  the simultaneous requirement for biological realism and stability is

$$1 < R_0 < (1 - 2a)^{-1/a}. \quad (28)$$

However, for  $0 < a < \frac{1}{2}$ ,  $1/(1 - 2a)^{-1/a} > 1$  and so from (28) there is a region of stability.

In the limit as  $a \rightarrow 0$ , (28) implies that biologically meaningful (i.e. where a positive equilibrium exists) instability is only possible if

$$R_0 > e^2 \quad (29)$$

(thereby extending the result obtained by Levin and Goodyear (1980)).

Similar reasoning gives some insight into the stability conditions for the Shepherd function. For  $0 < \nu < 1$  the derivative at equilibrium is always positive,

thus stability is guaranteed. For  $1 < \nu < 2$  the derivative at equilibrium is not necessarily positive, but

$$-1 < 1 - \nu + \frac{\nu}{R_0} \quad (30)$$

is always satisfied and stability is still assured. This condition guaranteeing stability can be written as

$$R_0 < \frac{\nu}{2 - \nu}. \quad (31)$$

As  $\nu \rightarrow 2$  from below this condition implies that stability occurs regardless of the value of  $R_0$ . However for  $\nu > 2$  the condition tells us nothing about stability.

The situations of interest for further analysis are those cases where instability is possible. These are the cases  $\gamma > -\frac{1}{2}$  for the Deriso-Schnute function and  $\nu > 2$  for the Shepherd function.

The local stability conditions given above only define a region in which stability is guaranteed; *not* the precise point at which bifurcation occurs (i.e. the mathematical conditions are only sufficient). A relatively straightforward definition of the transition point can be achieved by working with simplified versions of demographic models. As will become apparent, use of aggregated models also makes it easier to describe, in addition to points of bifurcation, the subdivision of the stability region according to whether such stability is monotonic or oscillatory.

### 3. Aggregated models

In subsections 3.1 and 3.2 we review and synthesize results obtained by Deriso (1980) and Schnute (1985). New results appear in subsections 3.3 and 3.4.

#### 3.1. A general aggregation growth equation

A simplified demographic model can be derived if fecundity beyond age-at-maturity,  $\tau$ , satisfies the difference relationship

$$b_{i+1} = c_1 b_i + c_2 b_{i-1}. \quad (32)$$

In this Eq. (32) there are two constants,  $c_1$  and  $c_2$ , and two initial conditions,  $b_\tau$  and  $b_{\tau-1}$ . At this stage Eq. (32) should be viewed as a flexible *ad hoc* regression equation for describing observed fecundity-at-age levels, subject to four regression variables (see Schnute (1985) for details).

Define

$$B_t = \sum_{i=\tau}^n w_i N_i(t) \quad (33)$$

where  $w_i$  is the average weight of an individual aged  $i$ , and  $\tau$  is the age-at-maturity (i.e.  $b_i = 0$ ,  $i = 1, \dots, \tau - 1$ ). Then  $B_t$  is the biomass of the breeding (adult) population at time  $t$ . (The reader should note that the time variable  $t$  appears in the subscript position for the gross biomass variable  $B$ , while the subscript  $i$  in  $N_i(t)$  still refers to age class. Both  $i$  and  $t$ , however, have the same units of time).

If individual fecundity is proportional to individual mass, which is often the case for mature fish,

$$b_i = \kappa w_i, \quad i = \tau, \dots, n \tag{34}$$

where  $w_i$  and  $\kappa$  are respectively individual mass-at-age and a proportionality constant, then growth follows the same model as fecundity changes. Therefore  $N_0(t)$ , the egg production variable, is proportional to population biomass, since from (3),

$$N_0(t) = \kappa \sum_{i=\tau}^n w_i N_i(t). \tag{35}$$

A conservation of mass statement for  $n \rightarrow \infty$  is

$$B_{t+1} = \sum_{i=\tau}^{\infty} w_i N_i(t+1) = \sum_{i=\tau}^{\infty} w_{i+1} N_{i+1}(t+1) + w_{\tau} N_{\tau}(t+1). \tag{36}$$

If adult survivorship,  $s$ , is independent of age or year (i.e.  $N_{i+1}(t+1) = sN_i(t)$ ,  $i = \tau, \dots, \infty$ ) then Eq. (36) can be rewritten as

$$B_{t+1} = s \sum_{i=\tau}^{\infty} w_{i+1} N_i(t) + w_{\tau} N_{\tau}(t+1). \tag{37}$$

Substitute  $[c_1 w_i + c_2 w_{i-1}]$  for  $w_{i+1}$  to obtain

$$B_{t+1} = c_1 s \sum_{i=\tau}^{\infty} w_i N_i(t) + c_2 s \sum_{i=\tau}^{\infty} w_{i-1} N_i(t) + w_{\tau} N_{\tau}(t+1). \tag{38}$$

If we now replace  $N_i(t)$  in the second summation term of (38) by  $sN_{i-1}(t-1)$  and use expression (33) we obtain

$$B_{t+1} = c_1 s B_t + c_2 s^2 B_{t-1} + c_2 s^2 w_{\tau-1} N_{\tau-1}(t-1) + w_{\tau} N_{\tau}(t+1). \tag{39}$$

From (3), (7), (8) and (9) note that

$$N_{\tau}(t+1) = l_{\tau} N_0(t-\tau+1) \phi[N_0(t-\tau+1)] \tag{40}$$

and

$$N_{\tau-1}(t-1) = l_{\tau-1} N_0(t-\tau) \phi[N_0(t-\tau)] \tag{41}$$

where  $\phi(N_0(t))$  is the density dependent egg survival factor and  $l_{\tau}$  is density independent survivorship from the age of zero to exactly  $\tau$  years. Since  $N_0 = \kappa B_t$ , then by defining

$$\psi(B) = \kappa \phi(\kappa B). \tag{42}$$

Equation (39) can finally be expressed in the form

$$B_{t+1} = c_1 s B_t + c_2 s^2 B_{t-1} + c_2 s^2 l_{\tau-1} w_{\tau-1} B_{t-\tau} \psi(B_{t-\tau}) + l_{\tau} w_{\tau} B_{t-\tau+1} \psi(B_{t-\tau+1}). \tag{43}$$

We do not describe the stability conditions for the model in this form. The formulation as it now stands (which is inspired by the special case derived by Deriso (1980)), however, is a useful extension of the Deriso model. Note that there are only 4 delay variables on the right-hand side of this equation (i.e.  $B_t$ ,

$B_{t-1}$ ,  $B_{t-\tau}$  and  $B_{t-\tau+1}$ ), compared to  $n$  for the disaggregated model (2). This reduced parameter space is of considerable importance for the regression analysis of observed data, since excessive parameterization causes a reduction in estimator efficiency.

### 3.2. The Schnute and Deriso forms

With fecundity proportional to body mass, (32) can be expressed in terms of  $w_i$ , as follows

$$w_{i+1} = c_1 w_i + c_2 w_{i-1}. \quad (44)$$

This equation has an equilibrium solution  $w^*$  if and only if  $c_1 + c_2 = 1$ . Let  $\rho = c_1 - 1 = -c_2$ . Then the characteristic equation associated with (44) is a quadratic,  $\lambda^2 - (1 + \rho)\lambda + \rho = 0$ , which has roots  $\lambda = 1$  and  $\lambda = \rho$ . Therefore  $w^*$  can at best be marginally stable, when  $|\rho| \leq 1$ . If we restrict ourselves to cases where (44) has an equilibrium (that is  $w_i$  does not grow without bound), then (44) becomes

$$w_{i+1} - w_i = \rho(w_i - w_{i-1}). \quad (45)$$

To rule out the possibility of decreasing body mass with increasing age, i.e. shrinking, we require  $\rho \geq 0$ . Thus, if there is to be no shrinking, and if the equilibrium body size is to be marginally stable, the necessary bounds on  $\rho$  are

$$0 \leq \rho \leq 1 \quad (46)$$

(see Schnute and Fournier (1980) for further details). Equation (45) is known as the Ford growth equation, and  $\rho$  is known as the Brody growth coefficient. Substituting  $1 + \rho$  for  $c_1$  and  $-\rho$  for  $c_2$  in Eq. (43), the population model becomes

$$B_{t+1} = (1 + \rho)sB_t - \rho s^2 B_{t-1} - \rho s^2 l_{\tau-1} w_{\tau-1} B_{t-\tau} \psi(B_{t-\tau}) + l_{\tau} w_{\tau} B_{t-\tau+1} \psi(B_{t-\tau+1}). \quad (47)$$

This result is identical in form to Eqs. (2.7) and (2.9) (p. 420 of Schnute (1985)). Deriso (1980) makes the simplifying assumption that  $w_{\tau-1} = 0$ . Therefore the Deriso model is

$$B_{t+1} = (1 + \rho)sB_t - \rho s^2 B_{t-1} + l_{\tau} w_{\tau} B_{t-\tau+1} \psi(B_{t-\tau+1}). \quad (48)$$

The classification of the behaviour of solutions to the Deriso model in the neighbourhood of an equilibrium will be described here, but first we define the equilibrium state of the model and the characteristic equation at equilibrium.

From Eq. (48) it follows that the equilibrium population biomass for Deriso's model,  $B^*$ , is

$$B^* = \psi^{-1}[(1-s)(1-\rho s)/l_{\tau} w_{\tau}] \quad (49)$$

provided that the inverse function  $\psi^{-1}(\cdot)$  exists. If  $\rho > 1/s$ , then  $(1-s)(1-\rho s)$  is negative, which implies that recruitment is negative. Therefore, for the equilibrium to be positive, it is necessary that  $\rho < 1/s$ . This constraint, however, is already satisfied by (46). The characteristic equation for the Deriso model in the absence of human exploitation is

$$\lambda^{\tau} - (1 + \rho)s\lambda^{\tau-1} + \rho s^2 \lambda^{\tau-2} - D = 0 \quad (50)$$

where the variable  $D$  is the slope of the recruitment function at equilibrium,

$$D = l_{\tau} w_{\tau} \frac{d}{dB} [B\psi(B)]|_{N_0=N_0^*} \quad (51)$$

(defining recruitment as the biomass of individuals aged  $\tau$  years).

Local stability properties for the Deriso model can be obtained by solving for the roots of the characteristic Eq. (50) and examining their real and imaginary parts.

### 3.3. Stability of the Deriso model

In Deriso (1978), the local stability analysis for a more general version of (47) is developed for the four cases  $\tau = 2, 3, 4$  and  $\tau \rightarrow \infty$ . The analysis in Deriso (1978) uses necessary and sufficient bounds on the moduli of roots of the characteristic equation (50) to establish sufficient local stability conditions. These conditions are standard conditions for roots of polynomials of order  $n$  to lie within the unit circle, as given in Marden (1966). In Deriso (1978) the bifurcation threshold is determined by numerically tracing a path through parameter space and finding the point at which a condition is first violated.

The above method has the disadvantage that it is not generally applicable to other values of  $\tau$ . It does also not lead to direct calculation of the imaginary and real parts of the dominant eigenvalue on the unit circle. The latter is needed if bifurcation periods are to be calculated.

Here we apply a method which is valid for any integral  $\tau$  value. Since the real and imaginary parts of the dominant eigenvalue on the unit circle are explicitly evaluated, bifurcation periods are easily obtained, whereas with Deriso's (1978) method, this is not possible. Finally, the analysis permits categorisation of the stability region as being either monotonic or oscillatory.

The stability/instability threshold is a function of the model parameters  $\tau, s, \rho$  and of the recruitment slope parameter  $D$ . Although we have focussed on stability as a function of  $D$ , equivalent statements are possible using one of the other parameters  $\tau, s, \rho$  as the operative variable.

An equilibrium is stable if all the eigenvalues of the system linearized around this equilibrium have moduli less than one. Within this regime of stability, if the dominant eigenvalue is real and positive, then the behaviour of the population as it returns to equilibrium following a disturbance is primarily a geometric (monotonic) decay, although the subdominant complex roots will cause some oscillations. If the dominant eigenvalue is negative, or complex, then the population oscillates as it approaches equilibrium. Instability sets in if the modulus of an eigenvalue exceeds 1. If a real eigenvalue exceeds 1 then the population will move away from the equilibrium in a predominantly geometric/monotonic fashion. If an eigenvalue decreases below  $-1$ , or the modulus of a complex conjugate set of roots exceeds 1, then oscillatory instability occurs.

The four categories of behaviour we seek to describe here are thus monotonic instability, monotonic stability, damped oscillations (stable) and undamped oscillations (unstable).

In order to describe the stability thresholds for Deriso's model, we identify conditions when the dominant eigenvalues lie on the unit circle. However, since the coefficients of  $\lambda^{-1}$  for the Perron form of the characteristic equation

$$(1 + \rho)s\lambda^{-1} - \rho s^2\lambda^{-2} - D\lambda^{-\tau} = 1 \quad (52)$$

can never all be positive, the Perron–Frobenius Theorem cannot be used to determine necessary and sufficient local stability conditions. The following is an extension of Levin and May’s (1976) analysis (in which they determine local stability conditions for a special case of Deriso’s model) to Deriso’s model.

*3.3.1. Transition from monotonic instability to stability.* We factorise the characteristic equation of the Deriso model to obtain

$$\lambda^{\tau-2}(\lambda - \rho s)(\lambda - s) = D. \quad (53)$$

When  $D = 0$ , either the root  $\lambda = s$  ( $0 < \rho < 1$ ) or  $\lambda = \rho s$  ( $1 < \rho < 1/s$ ) is dominant, since the other roots are all zero. As  $D$  increases, the values of these roots change. Does the dominant root at  $D = 0$  remain dominant for non-zero values of  $D$ ; that is, is it the first root to reach the unit circle with a value  $\lambda = 1$  when  $D = (1 - \rho s)(1 - s)$ ? To analyse this question we follow the approach taken by Levin and May (1976). Before doing so, note that the functional relationship between all the model parameters when an eigenvalue lies on the unit circle (when the modulus of an eigenvalue is unity) is described by the real and imaginary equations which result if  $\lambda$  is replaced by  $e^{i\theta}$  in the characteristic Eq. (53), i.e.

$$e^{i\theta\tau} - (1 + \rho)s e^{i\theta(\tau-1)} + \rho s^2 e^{i\theta(\tau-2)} = D \quad (54)$$

for which the real and imaginary parts respectively are

$$\cos \theta\tau - (1 + \rho)s \cos \theta(\tau-1) + \rho s^2 \cos \theta(\tau-2) = D \quad (55)$$

$$\sin \theta\tau - (1 + \rho)s \sin \theta(\tau-1) + \rho s^2 \sin \theta(\tau-2) = 0. \quad (56)$$

Any solution to the imaginary equation on  $0 < \theta < \pi$  has a companion on  $\pi < \theta < 2\pi$ , since for any solution  $\theta$  of the imaginary equation,  $2\pi - \theta$  is also a solution. Hence the roots are conjugate complex pairs. The value  $D$  is the same for either of the roots in the conjugate complex pair. Furthermore, the periodicity generated by a root with an angle  $\theta$  is exactly the same as that generated by a root with an angle of  $2\pi - \theta$  (Appendix A). Thus, without loss of generality, we restrict the analysis to the interval,  $0 \leq \theta < \pi$ .

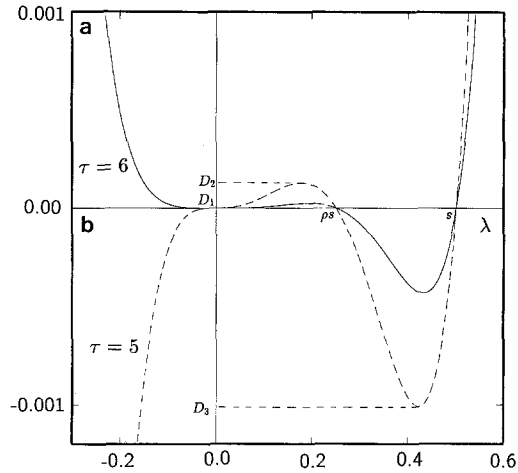
From the above, all the roots of the characteristic equation lie within the unit circle when  $D = 0$ .

First we observe that since the moduli of polynomial roots are continuous functions of the polynomial coefficients (Marden, 1966), the *moduli of roots of (53) are continuous functions of  $D$* .

Then, in Appendix B we show that if  $D$  is positive, the solution  $\theta$  is an increasing function of  $D$ . In particular as  $D$  increases from 0, the first time a solution  $\theta$  occurs in (53) must therefore correspond to  $\theta = 0$ ; that is the first root associated with (53) that crosses the unit circle is a real, positive root (since  $\theta = 0$ ).

Also, since a positive  $D$  value is an increasing function of  $\theta$ , for all values of  $0 < R < 1$  (where  $R$  is defined in Appendix B as the modulus of a root of (53)), the positive root is the first root to cross all circles with radii between  $s$  (or  $\rho s$  whichever is the largest positive root when  $D = 0$ ) and 1, as  $D$  increases (Fig. 2). Therefore the positive root is dominant for all its values between  $s$  (or  $\rho s$  whichever is larger at  $D = 0$ ) and 1.

**Fig. 2.** Two examples of  $D$  as a function of  $\lambda$  for  $\lambda$  real. **a**  $\tau = 6$  —  $D = \lambda^4(\lambda - \rho s)(\lambda - s)$ , **b**  $\tau = 5$  —  $D = \lambda^3(\lambda - \rho s)(\lambda - s)$ . In both cases  $s = 0.5$  and  $\rho = 0.5$ . These two curves are typical of all curves (with  $\tau$  either odd or even) with respect to the position of the two real roots, viz. 0,  $s$  and  $\rho s$ , and the position of the local maxima/minima, viz. two local minima — at  $D = D_1 = 0$  and  $D = D_3$  and a local maximum inbetween these two at  $D_2$



**3.3.2. Transition from monotonic stability to oscillating stability.** Let  $f(\lambda)$  be the left-hand side of Eq. (53), i.e.

$$f(\lambda) = \lambda^{\tau-2}(\lambda - \rho s)(\lambda - s). \tag{57}$$

For  $\tau \geq 3$  there are two basic forms, depending on whether  $\tau$  is even or odd. These are illustrated in Fig. 2. From this it follows that  $f(\lambda)$  has a positive root provided  $D < D_3$ . This point ( $D_3$ ) marks the transition between monotonic stability and oscillating stability, provided that this positive root is dominant between  $D = 0$  and  $D = D_3$ . To show this we need the fact that the moduli of all roots are continuous functions of  $D$ , and that when  $D = 0$  all roots lie within the unit circle. Also from Appendix B we conclude that when  $D$  is negative, then  $D$  is a decreasing function of  $\theta$ , if  $0 < \theta < \pi$ . If any complex root were to cross the circle with radius equal to the size of the positive root, then this would only be possible at a crossing point for the appropriate  $\theta$  value. But  $dD/d\theta < 0$  so this would necessarily have to be for some larger negative (larger in modulus) value of  $D$ . Therefore the positive root is dominant whenever it exists.

Thus the value of  $D$  at the transition from monotonic to oscillating stability is the largest negative value which still permits a positive real root. There are two critical values of  $D$  for which a real positive  $\lambda$  exists in Eq. (53); these are the local maximum and minimum of  $f(\lambda)$  that occur at  $D_2$  and  $D_3$  respectively. For  $D > D_2$ , however, we still have a dominant positive root, therefore  $D_3$  defines the value of  $D$  at which stability becomes oscillatory. The critical points occur at the roots of the derivative of  $D$  with respect to  $\lambda$ , i.e. the roots of  $g(\lambda)$  where

$$g(\lambda) = \tau \lambda^{\tau-1} - (1 + \rho)s(\tau - 1)\lambda^{\tau-2} + \rho s^2(\tau - 2)\lambda^{\tau-3}. \tag{58}$$

The largest positive root (i.e., corresponding to  $D_3$ ) is

$$\lambda = \frac{(1 + \rho)s(\tau - 1)}{2\tau} + \left[ \frac{(1 + \rho)^2 s^2 (\tau - 1)^2}{4\tau^2} - \frac{\rho s^2 (\tau - 2)}{\tau} \right]^{1/2} \tag{59}$$

and the value of  $D$  at which monotonic stability changes to oscillating stability is given by substituting this value into Eq. (53).

*3.3.3. Transition from oscillating stability to instability.* Once a positive root no longer exists, the behaviour of the linearized system is dominated by either negative real roots, or complex roots, i.e. its behaviour becomes oscillatory. This oscillating behaviour is initially locally stable, however at some point in the parameter space oscillating instability sets in. The transition occurs when the dominant eigenvalue crosses the unit circle. All roots lie within the unit circle when  $D = D_3$  (the dominant eigenvalue,  $\lambda_0$ , lies between  $s$  and  $\rho s$ ). Again, solutions of the characteristic equation on the unit circle give the values of  $D$  and  $\theta$  where the unit circle *may be crossed*. It is necessary to invoke the continuity of all moduli with respect to  $D$ , and the negativity of  $dD/d\theta$  when  $D$  is negative.

Therefore, as  $D$  decreases, the first crossing of the unit circle occurs at the smallest absolute value of  $D$  defining a crossing point. From Appendix B, this corresponds to a root on the unit circle with the smallest absolute value of  $\theta$  apart from zero ( $\theta = 0$  corresponds to a real positive root—this cannot exist if  $D < D_3$ ).

The transcendental equation for solutions of the characteristic equation on the unit circle can be solved numerically, using the imaginary part of the characteristic Eq. (56) on the unit circle to obtain the bifurcating value of  $\theta$ , and obtaining  $D$  from the real part (55). We applied Newton's method to numerically search for the solution to Eq. (56) to find the smallest non-zero root  $\theta$  of  $y(\theta, \rho, s, \tau)$  for given values of  $\rho$ ,  $s$  and  $\tau$ , where

$$y(\theta, \rho, s, \tau) = \frac{\sin \tau\theta + \rho s^2 \sin \theta(\tau-2)}{(1+\rho) \sin(\tau-1)\theta} - s. \quad (60)$$

The critical values of  $D$  for bifurcation to monotonic instability and oscillating instability, and the subdivision of the region of stability between regions of monotonic and oscillating stability, are illustrated in Fig. 3a-e, for  $s = 0, 0.2, \dots, 1.0, 0 < \rho < 1$  and  $\tau = 2, 3, \dots, 6$ . The associated bifurcation periods are set out in Fig. 4a-e.

*3.3.4. The cases  $\tau = 1, \tau = 2, \tau \rightarrow \infty$ .* For both  $\tau = 1$  and  $\tau = 2$  the characteristic equation is a quadratic function. The quadratic for  $\tau = 1$  is

$$\lambda^2 - [(1+\rho)s + D]\lambda + \rho s^2 = 0. \quad (61)$$

For  $\tau = 2$  it is

$$\lambda^2 - (1+\rho)s\lambda + \rho s^2 - D = 0. \quad (62)$$

The local stability analysis involves an analysis of the size of the two moduli corresponding to the two roots of a quadratic function. Stability categories as functions of model parameters are presented in Table 1.

To analyse the case  $\tau \rightarrow \infty$ , consider the sine functions (a)  $\sin \theta\tau$ , (b)  $-(1+\rho)s \sin \theta(\tau-1)$ , and (c)  $\rho s^2 \sin \theta(\tau-2)$  in the imaginary part (56) of the characteristic equation. They are all zero, when  $\theta = 0$ . They respectively return to zero when  $\theta = \pi/\tau, \pi/(\tau-1), \pi/(\tau-2)$ . The function (a) + (c) crosses zero somewhere between  $\pi/\tau$  and  $\pi/(\tau-2)$ , say at  $\delta\pi$ , which is not necessarily the point  $\pi/(\tau-1)$  at which (b) crosses 0. Irrespective of whether  $\delta\pi$  is greater or less than  $\pi/(\tau-1)$  and  $(1+\rho s^2)$  is greater or less than  $s(1+\rho)$ , the imaginary part of Eq. (56) will

have a zero somewhere *before* the sine functions (a), (b), and (c) all cross zero for the second time as  $\theta$  increases from zero: i.e. before  $2(\pi/(\tau-2))$ . Therefore, the smallest non-zero  $\theta$  solution to Eq. (56), say  $\theta_s$ , is bounded by  $2(\pi/(\tau-2))$ . Since  $\lim_{\tau \rightarrow \infty} 2(\pi/(\tau-2)) = 0$ , then  $\lim_{\tau \rightarrow \infty} \theta_s = 0$ , and  $\lim_{\tau \rightarrow \infty} \cos[n\theta_s] = 1$  for all finite  $n$ .

From Eq. (B5) (see Appendix B) we have, on the unit circle (i.e. conditions for bifurcation) that

$$\lim_{\tau \rightarrow \infty} D^2(\theta_s)|_{R=1} = [(1-\rho s)(1-s)]^2. \tag{63}$$

Therefore in the limit  $D$  could be  $D^+ = (1-\rho s)(1-s)$  or  $D^- = -(1-\rho s)(1-s)$ . When  $D = D^+$  the characteristic Eq. (53) still has a positive root, so the limiting case at bifurcation to oscillating instabilities must be  $D^-$ , i.e.

$$\lim_{\tau \rightarrow \infty} D(\theta_s)|_{R=1} = -(1-\rho s)(1-s). \tag{64}$$

The same result is presented in Deriso (1978).

### 3.4. The Allen-Clark model

A special case of the Deriso model is the case,  $\rho = 0$ , which is the assumption that no further increase in body mass  $w_i$  occurs beyond the age at which maturity is attained: i.e. this model has the form

$$B_{i+1} = sB_i + w_l B_{i-\tau+1} \psi(B_{i-\tau+1}). \tag{65}$$

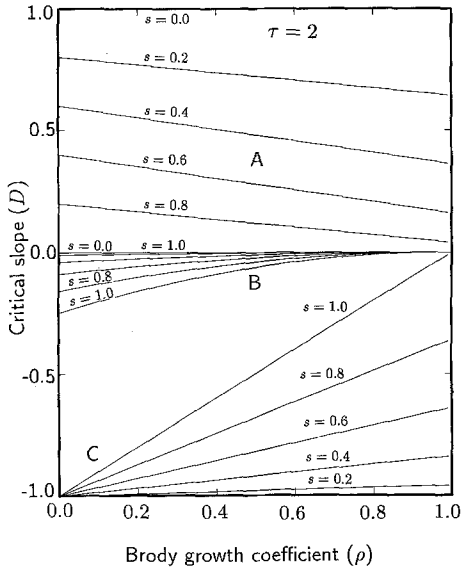
The local stability properties for this model are discussed by Clark (1976), and some results for global stability are given in Fisher and Goh (1984). Clark cites an earlier application of the model by Allen (1970). We thus refer to it as the Allen-Clark model. The local stability results obtained for the Deriso model are applicable to this model, when  $\rho = 0$ . The following is a summary of local stability results for the Allen-Clark model.

**3.4.1 Transition from monotonic stability to oscillating stability.** The first derivation is of the transition point from monotonic stability to oscillating stability, assuming that the former transition from monotonic stability is easily obtained from the Deriso model as a special case.

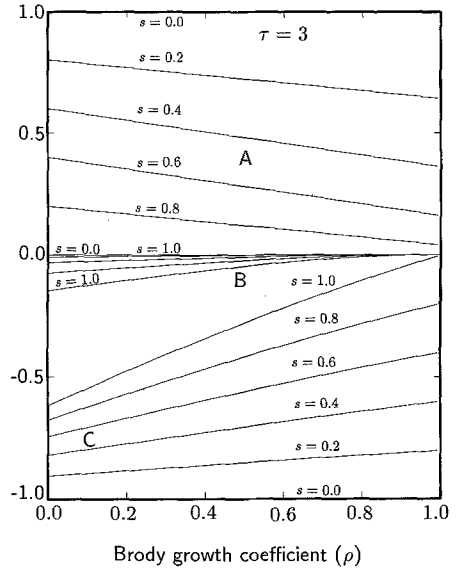
By the Perron-Frobenius Theorem, the dominant eigenvalue of the characteristic equation for the Allen-Clark model

$$\lambda^\tau - s\lambda^{\tau-1} - D = 0 \tag{66}$$

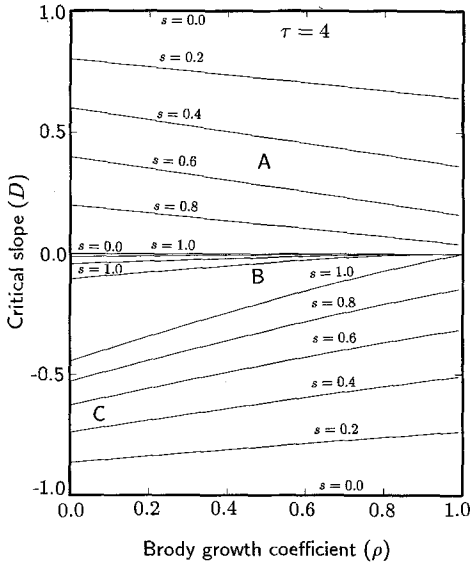
is real and positive if  $D > 0$ . Since a real positive root exceeds unity when  $D = 1 - s$ , the region  $0 < D < 1 - s$  is a region of monotonic stability. However, there is a region  $D_l < D < 0$  for which there are still positive real roots to the characteristic equation. Therefore  $D = 0$  does not necessarily define the transition to oscillating instability. When  $D$  is zero,  $\lambda = 0$  and  $\lambda = s$ ; and  $D$  is negative for  $\lambda \in [0, s]$ . Therefore the smallest value of  $D$  which still permits a real positive solution to



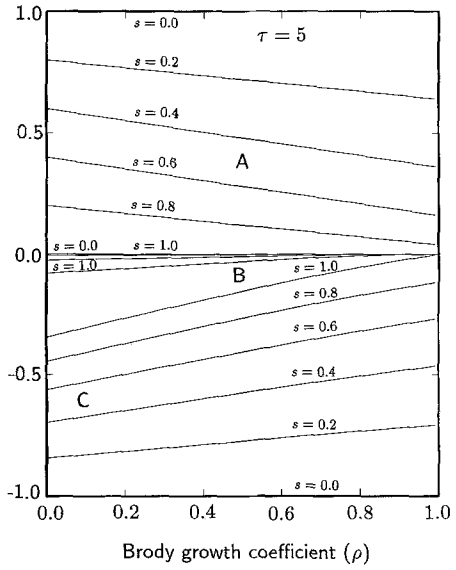
a



b

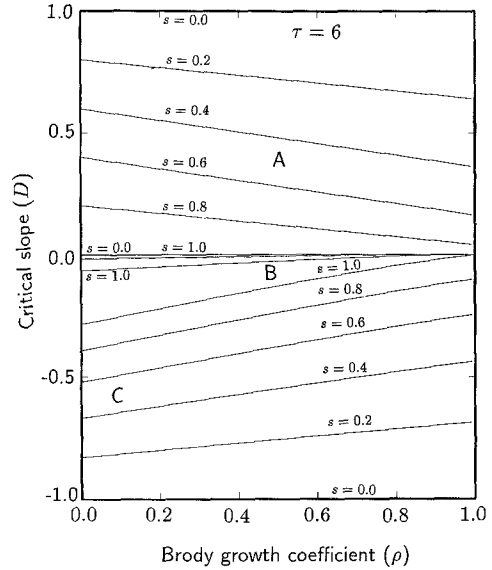


c



d

**Fig. 3a-e.** Critical values of  $D$  at bifurcation to monotonic instability (lines approximately parallel near  $A$ ), to oscillating instability (lines diverging near  $C$  or apparently from some point to the left of  $C$ ) and the point of transition from monotonic stability to oscillating stability (lines converging towards  $B$  and further right) for the Deriso model (48) for different values of the age-at-maturity,  $\tau$ . Note that line  $A$  for  $s=0.0$  coincides with the upper border of the figure, and line  $A$ ,  $s=1.0$ , coincides with line  $B$ ,  $s=0.0$



e

**Table 1.** Stability regimes for Deriso’s model for  $D$  as a function of  $s$  and  $\rho$ , with  $\tau=1$  and  $\tau=2$

$\tau$	Range	Behaviour
1	$D > 1 - (1 + \rho)s + \rho s^2$	Monotonically unstable
	$2\sqrt{\rho}s - (1 + \rho)s < D < 1 - (1 + \rho)s + \rho s^2$	Monotonically stable
	$-2\sqrt{\rho}s - (1 + \rho)s < D < 2\sqrt{\rho}s - (1 + \rho)s$	Stable oscillations ( $\lambda$ complex)
	$-1 - (1 + \rho)s - \rho s^2 < D < -2\sqrt{\rho}s - (1 + \rho)s$	Stable oscillations ( $\lambda$ negative)
	$-1 - (1 + \rho)s - \rho s^2 > D$	Unstable oscillations
2	$D > 1 - (1 + \rho)s + \rho s^2$	Monotonic unstable
	$\rho s^2 - 1/4(1 + \rho)^2 s^2 < D < 1 - (1 + \rho)s + \rho s^2$	Monotonic stable
	$\rho s^2 - < D < \rho s^2 - 1/4(1 + \rho)^2 s^2$	Stable oscillations ( $\lambda$ complex)
	$\rho s^2 - 1 > D$	Unstable oscillations

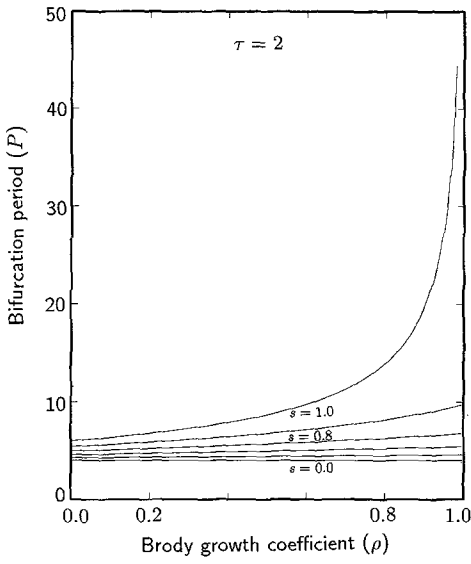
the characteristic equation must be a critical point for  $\lambda$  somewhere between 0 and  $s$ . The positive root of the derivative of  $D$  with respect to  $\lambda$  is easily shown to be

$$\lambda = \frac{s(\tau - 1)}{\tau} \tag{67}$$

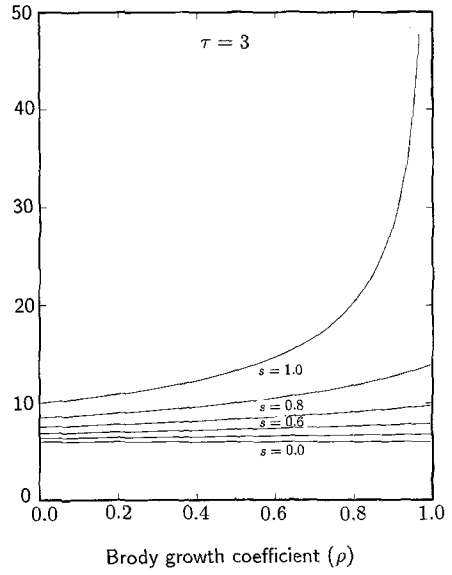
and the associated value of  $D_l$  is

$$D_l = -\frac{(\tau - 1)^{\tau - 1} s^\tau}{\tau^\tau} \tag{68}$$

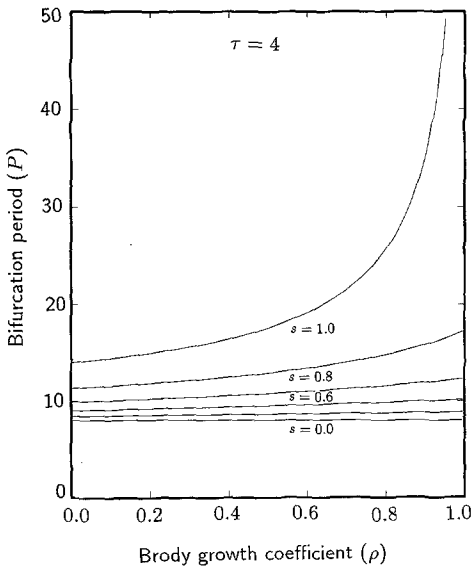
The proof that the positive real root is dominant for  $D_l < D < 0$  follows as a special case of the discussion for Deriso’s model presented earlier.



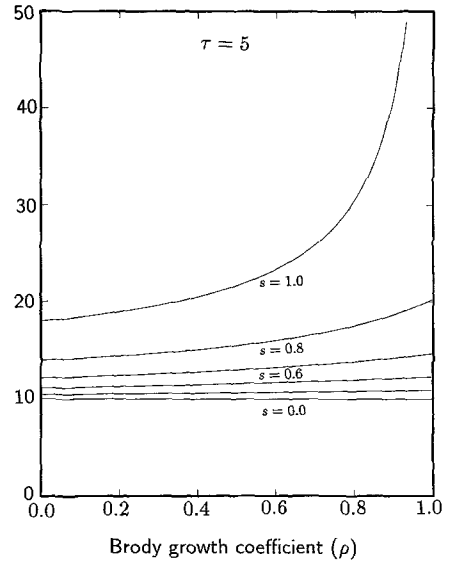
a



b



c



d

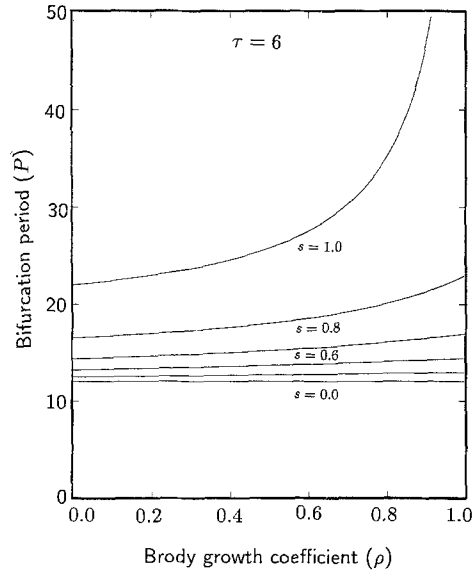


Fig. 4a-e. Bifurcation periods for the Deriso model (48) in units of the time interval (normally one year for annually breeding animals), for  $5\tau$  values and 6 survivorship levels

3.4.2. *Transition from oscillating stability to instability.* Levin and May (1976) presented the local stability analysis for the general model

$$B_{t+1} = B_t F(B_{t-\tau+1}). \tag{69}$$

The characteristic equation for this model is identical to (66) with  $s = 1$ . Therefore, stability results presented in Levin and May (1976) are applicable to the Allen-Clark model for  $s = 1$ . Here we extend these results to the interval  $s \in [0, 1]$ .

Levin and May (1976) were able to obtain an analytical expression for the transition to oscillating instability. They solved the transcendental equation for the characteristic equation, to show that the values of  $D$  on the unit circle at bifurcation are

$$D = -2 \cos(\theta(\tau - 1)) \tag{70}$$

where

$$\theta = \frac{(2n + 1)\pi}{2\tau - 1}, \quad n = 0, 1, 2, \dots \tag{71}$$

For  $D < 0$ , the smallest absolute value of  $D$  associated with a root on the unit circle is the value obtained when  $n = 0$  in (71), i.e.

$$D = -2 \cos \left[ \frac{\pi(\tau - 1)}{2\tau - 1} \right]. \tag{72}$$

Therefore, since this is the first point on the unit circle as  $D$  decreases from  $D = 0$ , this point, viz. the value of  $D$  corresponding to the smallest  $\theta$  value which is a solution to the imaginary part of the characteristic equation, is also the point marking the transition to oscillating instability.

This result generalises to  $s \in [0, 1]$  if one can show that there is no point in  $s \in [0, 1]$  at which the root with smallest  $\theta$  value loses dominance on the unit circle. This holds if on the unity circle a given value of  $D$  can only be associated with a single unique value of  $\theta$  for  $\theta \in [0, \tau]$  and  $s \in [0, 1]$ .

When  $R = 1$  and  $\rho = 0$  then Eq. (B5) (see Appendix B) becomes

$$D^2 = 1 + s^2 - 2s \cos \theta. \quad (73)$$

Therefore  $D^2$  is a strictly increasing function of  $\theta$ , for  $\theta \in [0, \tau]$ , from which it follows that when  $D < 0$  there is a unique value of  $\theta$  for every  $D$  value. Therefore the root on the unit circle with the smallest value of  $\theta$  always marks the bifurcation threshold for  $s \in [0, 1]$ .

**3.4.3. Numerical solution for  $\theta$  and  $D$  at bifurcation,  $D < 0$ .** When  $\rho = 0$ , there are four variables in the transcendental equation (54) at the unit circle;  $\theta$ ,  $\tau$ ,  $s$  and  $D$ . We determine  $D$  and  $\theta$  as functions of given values of  $\tau$  and  $s$ .

The value of  $D$  at bifurcation to oscillating instability can be calculated by numerically solving for the smallest non-zero solution of  $\theta$  to Eq. (56) for  $\theta$  between 0 and  $\pi$  and for  $\rho = 0$ . Results presented here were obtained using Newton's method to solve for the roots of  $y(\theta, s, \tau)$  where

$$y(\theta, s, \tau) = \frac{\sin \theta \tau}{\sin \theta(\tau - 1)} - s \quad (74)$$

for given values of  $s$  and  $\tau$ , and then calculating  $D$  from Eq. (55). This is the same as Clark's (1976) procedure. However we provide a more complete summary of the stability threshold values for  $D$  as a function of  $s$  and  $\tau$ .

The limiting case,  $\tau \rightarrow \infty$ , by earlier arguments for the Deriso model, bifurcates when  $D = -1 + s$ . Values of  $D$  for bifurcation to oscillating instability are shown as a function of  $s$  and for  $\tau$  values from 1 to 11 in Fig. 5. The same figure also shows the point of transition from dominant monotonic stability to dominant oscillating stability as a function of  $s$  and  $\tau$ , and the point at which monotonic instability first occurs ( $D = 1 - s$ ).

**3.4.4. Bifurcation periods.** Bifurcation periods are obtained directly from the angle of the dominant eigenvalue at the threshold of instability. The results for the limits  $s \rightarrow 0$  and  $s \rightarrow 1$  give the lower and upper bounds of the oscillation period. As  $s \rightarrow 0$ , Eq. (56) becomes (with  $\rho = 0$ )

$$\sin \theta \tau = 0 \quad (75)$$

which has as smallest non-zero solution (i.e. lowest frequency of oscillation),  $\theta = \pi/\tau$ . The associated bifurcation period is  $2\tau$ , i.e. twice the age-at-maturity.

As  $s \rightarrow 1$  Eq. (56) becomes

$$\sin \theta \tau = \sin \theta(\tau - 1). \quad (76)$$

The smallest solution of  $\theta$  to this equation lies between  $\pi/2\tau$  and  $\pi/2(\tau - 1)$  and so  $\theta(\tau - 1)$  and  $\theta\tau$  must lie in the first and second quadrants,  $[0, \pi/2]$  and  $[\pi/2, \pi]$  respectively. From (76) it follows that  $\pi - \theta\tau = \theta(\tau - 1)$ ; that is,

$$\theta = \frac{\pi}{2\tau - 1} \quad (77)$$

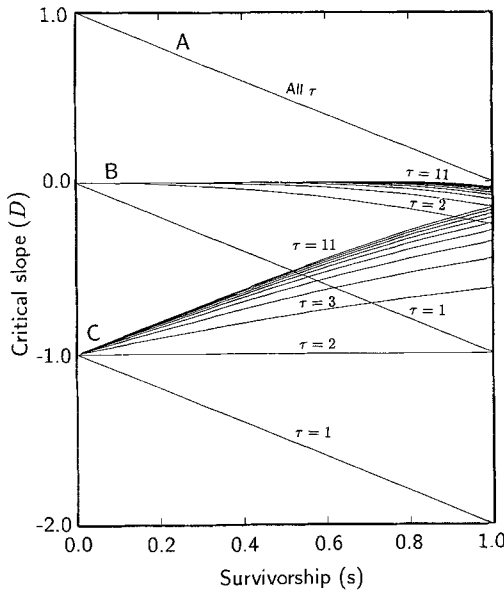


**Fig. 5.** Critical values of  $D$  at bifurcation to monotonic instability (line  $A$  — independent of  $\tau$ ), to oscillating instability (lines diverging to the right from  $C$ ) and the point of transition from dominant monotonic stability to dominant oscillating stability (lines diverging to the right from  $B$ ) for the Allen-Clark model (65) as a function of  $s$  between 0 and 1 and  $\tau$  between 1 (smallest possible) and 11 (close to the limit for  $\tau \rightarrow \infty$ )

which is a result obtained by Levin and May (1976). This corresponds to a bifurcation period of  $4\tau - 2$ . Therefore a continuous increase in  $s$  from  $0 \rightarrow 1$  is accompanied by a continuous increase in the bifurcation period, from  $2\tau$  to  $4\tau - 2$ . The numerically determined bifurcation periods for  $0 < s < 1$  for  $\tau$  from  $2 \rightarrow 11$  and  $s$  from  $0 \rightarrow 1$  are shown in Fig. 6. When  $\tau = 1$  the bifurcation period is 2 years for all  $s$ .

3.4.5. *The special cases  $\tau = 1$  and  $\tau = 2$ .* For these cases, the characteristic equation is ( $\tau = 1$ )

$$\lambda = s + D \tag{78}$$

and ( $\tau = 2$ )

$$\lambda^2 - s\lambda - D = 0. \tag{79}$$

Stability categories are obtained by examining the roots of a linear and a quadratic function, and the results are summarised in Table 2.

This completes the categorization of the deterministic stability states in the Deriso and Allen-Clark models without considering the effects of exploitation. For deterministic systems which are observed with some measurement error, the problem of recognizing instability arises. In the next section we discuss the problem of identifying instability in the unexploited population from data gathered in the field or from statistics associated with the harvesting process (e.g.

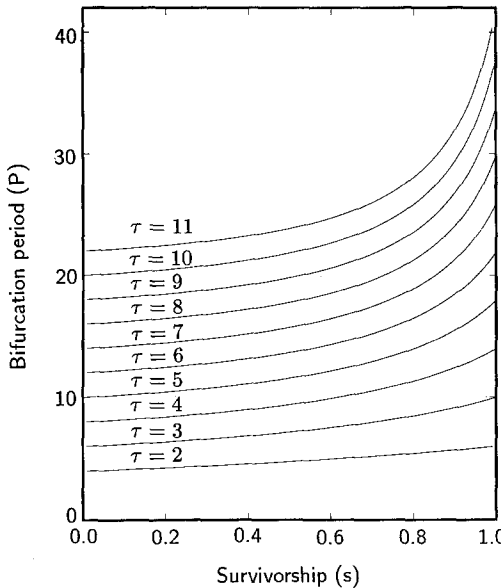


Fig. 6. Periods at bifurcation to oscillating instability for the Allen–Clark model (65), as a function of the  $s$  and  $\tau$  values considered in Fig. 5. At the extremums,  $s=0$  and  $s=1$ , the bifurcation periods are  $2\tau$  and  $4\tau-2$  respectively. The case,  $\tau=1$ , is not shown, but the bifurcation period is two years

catch statistics). We assume however that the underlying population dynamics is perfectly deterministic.

#### 4. Recognizing deterministic instability

The possibility that sustained oscillations caused by internal factors occur in marine populations has been raised recently by Deriso et al. (1985), as one of a number of competing hypotheses for explaining Pacific halibut dynamics. To be

Table 2. Stability regimes for the Allen–Clark model for  $D$  as a function of  $s$ , and for the special cases  $\tau=1$  and  $\tau=2$

$\tau$	Range	Behaviour
1	$D > 1-s$	Monotonically unstable
	$1-s > D > -s$	Monotonically stable
	$-s > D > -1-s$	Stable oscillations
	$-1-s > D$	Unstable oscillations
2	$D > 1-s$	Monotonically unstable
	$1-s > D > -\frac{s^2}{4}$	Monotonically stable
	$-\frac{s^2}{4} > D > -1$	Stable oscillations
	$-1 > D$	Unstable oscillations

able to resolve such debates in favour of a density dependent oscillation mechanism, available data must be used as the basis of a stability analysis of the equilibrium or equilibria.

We will restrict ourselves to an analysis of the case where population dynamics is perfectly deterministic, but population densities are observed with error. We also restrict the analysis to examining the properties of the unexploited system. If the survival parameter  $s$ , growth parameter  $\rho$ , and age-at-maturity  $\tau$  are all known exactly, then only  $D$  need be estimated to determine stability state.

The estimation of  $D$  for the unexploited population is complicated by the limited range of available data. Typically the data are clustered inbetween the origin and the unexploited equilibrium point on a stock recruitment plot (Fig. 1). The slope of the recruitment function at equilibrium can therefore only be obtained by extrapolating the fitted curve outside the region of observed data. Secondly, the estimate of  $D$  will usually be both imprecise (because of variance) and inaccurate (because of bias).

Walters and Ludwig (1981) consider a regression analysis of the Ricker function

$$R_{t+1} = \alpha S_{t-\tau+1} e^{-\beta S_{t-\tau+1}} \tag{80}$$

for the case  $\tau = 1$ , where  $R_t$  is recruitment in year  $t$  and  $B_t$  is the spawning biomass in year  $t$ . Define  $\hat{R}_t$  and  $\hat{B}_t$  to be the measured recruitment and spawning biomass levels respectively, while  $R_t$  and  $B_t$  are the associated actual (i.e. true) values. We assume that  $n$  pairs of points  $(R_t, B_{t-\tau})$  (e.g.  $t = \tau, \dots, n - 1 + \tau$ ) are available for the purpose of estimating  $\alpha$  and  $\beta$  using regression techniques.

In their analysis Walters and Ludwig (1981) estimate the bias induced in the estimate of  $\beta$  if there are measurement errors in both  $\hat{R}_t$  and  $\hat{B}_t$ , and if a simple linear regression of  $\ln(\hat{R}_t)/(\hat{B}_{t-\tau})$  versus  $\hat{B}_{t-\tau}$  is used to estimate the Ricker recruitment parameters  $\alpha$  and  $\beta$  (note: recruitment in year  $t$  is causally related to spawning biomass in year  $t - \tau$ ).

The slope of the recruitment function at unexploited equilibrium ( $D$ ) is independent of  $\beta$ . The value of  $\alpha$ , which is functionally related to  $D$  will be biased under certain circumstances if  $\beta$  is biased.

Walters and Ludwig (1981) derived an expression for the asymptotic (i.e. as  $n \rightarrow \infty$ ) bias in  $\hat{\beta}$ , which is

$$\hat{\beta} - \beta = -\beta \left[ (1 - 1/\mu^3) + \frac{1 - 1/\mu^2}{\mu} \frac{\bar{B}^2}{C_{BB}} \right] + \sigma_v^2 \frac{\bar{B}}{C_{BB}} \tag{81}$$

where  $\hat{\beta}$  is the estimate of the true density dependent parameter  $\beta$ ,  $\sigma_v^2$  is the variance of the logarithm of any recruitment or spawning biomass estimate with respect to the true value (these logarithms are assumed to be normally distributed),  $\mu$  is the asymptotic bias correction factor (for log-normal measurement noise in the recruitment and adult biomass estimates,  $\mu = e^{\sigma^2/2} > 1$ ,  $\bar{B}$  is the mean of all adult biomass estimates, taken from observations made over a period of  $n$  years, and  $C_{BB}$  is the total variance of all adult biomass estimates.

As an example, we consider an Allen-Clark model of an unexploited population with Ricker recruitment.

$$B_{t+1} = sB_t + \alpha B_{t-\tau+1} e^{-\beta B_{t-\tau+1}}. \tag{82}$$

The equilibrium biomass,  $B^*$ , is given by

$$B^* = \frac{1}{\beta} \ln \left[ \frac{\alpha}{1-s} \right], \quad (83)$$

and  $D$  can be written in the form

$$D = (1-s)(1-\beta B^*). \quad (84)$$

If  $s$  and  $B^*$  are fixed, then  $D$  is a decreasing function of  $\beta$ . Therefore, larger  $\beta$  values would lead to a greater chance of the equilibrium  $B^*$  being locally unstable.

Appendix C gives an estimate of the bias in  $D$  when spawning biomass and recruitment are obtained from independent estimates with equal lognormal error variances. The bias ( $\hat{D} - D$ ) is

$$(\hat{D} - D) = -(1-s)(\hat{\beta} - \beta)\bar{B}. \quad (85)$$

Dynamic instability definitely occurs for some sufficiently negative  $D$ , which from (84) occurs for some sufficiently large and positive  $\beta$ . Further, when  $\beta$  is sufficiently large and positive, then from (83) and Walters and Ludwig (1981) ( $\hat{\beta} - \beta < 0$ , and therefore from (85),  $(\hat{D} - D) > 0$ ). Since  $D < 0$  this implies that  $|\hat{D}| < |D|$ , and hence when a system is locally unstable and  $\beta$  is sufficiently large and positive, parameter estimates will erroneously indicate local stability.

Further complications with assessing the stability state of deterministic systems arise. Consider the following Deriso model subject to a constant catch rate  $C$  (refer to Deriso (1980) for the derivation of the catch equation) in which  $\tau = 2$ ,  $\rho = 0.1$ ,  $s = 0.6$  and  $\psi$  (see 42) is exponential so that there is a Ricker recruitment function:

$$B_{t+1} = [1.1][0.6](B_t - C) - (0.1)(0.6)^2 \left[ \frac{B_t - C}{B_t} \right] (B_{t-1} - C) + 9(B_{t-1} - C) e^{-[B_{t-1} - C]}. \quad (86)$$

Suppose the constant catch harvested each year is half of  $MSY$ , i.e.

$$C = \frac{MSY}{2} = 1.494. \quad (87)$$

This model has an unstable oscillatory equilibrium. Figure 7 shows a typical biomass trajectory of 280 year duration. The parameters used in (86) represent a sardine-like population. If all the system parameters apart from the Ricker function parameters are shown, then these can be estimated from the stock recruit regression analysis. The stock-recruit plot is obtained by plotting  $y$ , the recruitment biomass

$$y = B_{t+1} - [1.1][0.6](B_t - C) + (0.1)(0.6)^2(B_{t-1} - C) \left[ \frac{B_t - C}{B_t} \right] \quad (88)$$

against  $x$ , the spawning biomass

$$x = B_{t-1} - C. \quad (89)$$

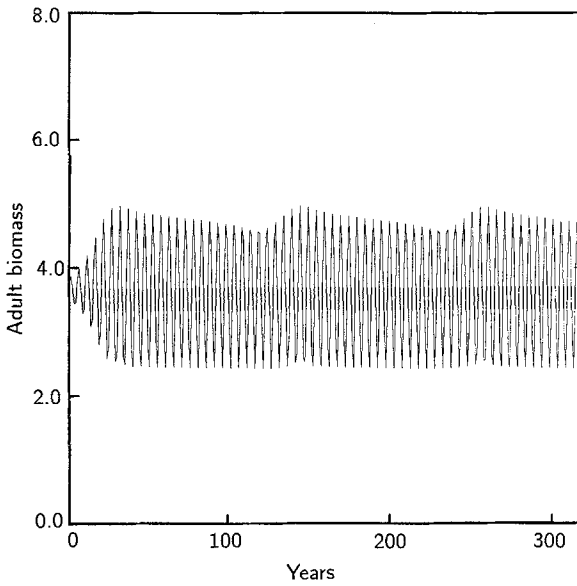


**Fig. 7.** A biomass trajectory for a fish population which has survivorship ( $s = 0.6$ ), growth rate ( $\rho = 0.1$ ) and age-at-maturity ( $\tau = 2$ ) similar to a sardine population, subject to a constant catch each year of  $MSY/2$ . The value of  $\alpha$  (see Eq. (82)) for the stock/recruit relationship was chosen so that the static equilibrium is locally unstable ( $\alpha = 9$ ). The trajectory was started very close to this unstable equilibrium point

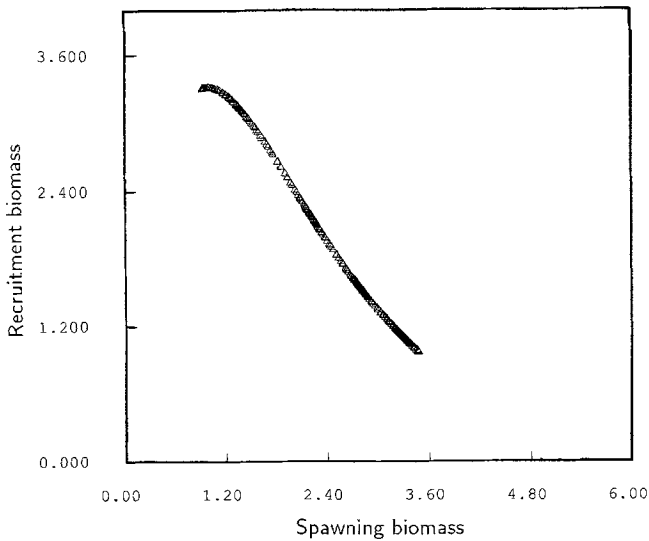


**Fig. 8.** Recruitment biomass versus adult biomass (after the harvest) for the last 280 years of data shown in Fig. 7. It is assumed that all the biomass values, the constant catch, and  $s$ ,  $\rho$  and  $\tau$  are exactly known and correctly specified

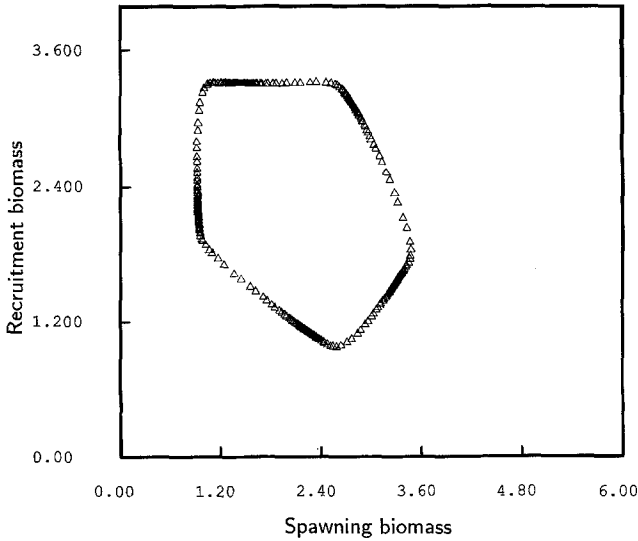


**Fig. 9.** Estimated recruitment biomass versus spawning biomass for the data shown in Fig. 7 (last 280 years). All the biomass values, the constant catch, and  $s$  and  $\rho$  are known exactly, however the value specified for  $\tau$  is incorrect, being 3 years rather than the correct value of 2 years

This plot (shown in Fig. 8) gives a good definition of part of the recruitment function. Because the system is dynamically unstable, it moves along a path, or attractor in some higher dimension coordinate system (see for example Guckenheimer et al (1977) or Schaffer (1984). The stock-recruit regression is the projection of the attractor which describes the shape of the recruitment function. If the system parameters which are used to calculate the recruitment biomass are incorrect then the resultant projection is not necessarily the desired projection of the recruitment function. For example, Fig. 9 shows the stock recruit relationship for the Deriso model described by Eq. (86) that would result if the value of  $\tau$  is erroneously assumed to be 3 years rather than the correct value of 2 years. There is now considerable "scatter" in the stock recruit plot. The scatter is perfectly deterministic, but achieves the same "smearing out" of the stock-recruit plot as do observation errors. This might also result in biases in  $\hat{D}$ , and hence cause a failure to recognise dynamic instability.

## 5. Discussion

From our analysis of the linearized system associated with density-dependent Leslie models considered here we obtain a condition essentially of the form

$$-\frac{1}{R_0} \leq k \leq \frac{1}{R_0}$$

where  $R_0$  is the density-independent reproductive value of the population and  $k$  is the slope of the stock recruitment function at an equilibrium. This condition is sufficient to guarantee local stability of the equilibrium being considered. The

transition to monotonic stability always lies at  $k = 1/R_0$ , but bifurcation to oscillating instability is generally beyond  $k = -1/R_0$ . For the case of the aggregated Deriso model, however, we are able to derive both necessary and sufficient conditions for local stability.

The results discussed here provide two tools for the analysis of real systems. These are the stability conditions themselves, and the period of oscillations at the bifurcation threshold (the bifurcation period). From experience we assume that the bifurcation period is a good approximation to the period generated by the non-linear dynamics. There are nevertheless several approaches that can be used to analyse how the dynamics change for values of  $D$  beyond the critical value at bifurcation. One of these is a straightforward simulation of the dynamics. This is only useful for specific situations. Another approach, reported in May (1974) and Guckenheimer et al. (1977), examines the stability of periodic states. Finally Tuljapurkar (1986) and Wachter (1987) analyse the period of oscillation for the nonlinear system by expressing it as an expansion in terms of the conditions prevailing at the point of bifurcation.

In terms of trying to understand the behaviour of dynamic systems from data, we showed for the Ricker recruitment function that observation errors can result in a failure to recognise deterministic instability. Apart from the specific effect of observation errors, there may be additional confounding effects if, for example, the incorrect time delay is used in the stock recruit regression. These problems (Figs. 7 and 8) may also arise if the age-at-maturity and age-at-recruitment are very different. In this case a more complex population model is required. The stock-recruit regression is very sensitive to the time-delay variable. Our example suggests that this parameter should be free during the regression calculation, although since  $\tau$  is discontinuous a special treatment is necessary. Failure to specify  $\tau$  correctly leads to exotic nonlinear behaviour on the stock-recruit plot.

The results obtained here provide a link between a number of discrete mathematical models used in ecological modelling. The analysis of discrete systems can be complex. The work presented here provides insight into the behaviour of a broad class of single species models that have application in resource management. Here we highlighted oscillating instabilities as a factor causing fish recruitment variability. Such dynamic instabilities may play a role in other variable resource systems.

*Acknowledgements.* We are indebted to three anonymous reviewers for their helpful comments. This work was supported by a South African CSIR FRD post-doctoral fellowship to MOB, NSF grant DMS-8511717 to WMG and an Alfred P. Sloan Foundation Grant 86-6-18 to Ken Wachter and WMG.

## Appendix A: Bifurcation period

When the system bifurcates to a state of oscillating instability, the modulus of the dominant pair of eigenvalues is on the unit circle. The two eigenvalues are  $\exp(i\theta)$  and  $\exp(i(2\pi - \theta))$ . The dynamics of the linearised system is dominated by these two roots, and the form of the dynamics is

$$B_t - B^* = C_1 e^{i\theta t} + C_2 e^{i(2\pi - \theta)t} \quad (\text{A1})$$

where the constants  $C_1$  and  $C_2$  depend on initial conditions, and where  $t = 1, 2, 3, \dots$ . The term  $C_1 e^{i\theta t}$  returns to the same value whenever  $\theta t = 2n\pi$  for  $n = 0, 1, 2, \dots$  and the time interval between two like values is  $2\pi/\theta$ , which is the period of oscillation. The other term is equivalently written as  $C_2 e^{i2\pi t} e^{-i\theta t}$ , which reduces to  $C_2 e^{-i\theta t}$  when  $i$  and  $t$  are positive integers. Since  $e^{-i\theta t}$  also oscillates with period  $2\pi/\theta$ , the bifurcation period is  $2\pi/\theta$ .

**Appendix B:  $\theta$  is an increasing function of  $D$  for all  $0 < \theta < \pi$  and for all circles with radii,  $R > 0$**

The characteristic equation can be rewritten in the form

$$\lambda - (1 + \rho)s + \rho s^2 \lambda^{-1} - D \lambda^{-(\tau-1)} = 0. \tag{B1}$$

Replacing  $\lambda$  by  $\text{Re}^{i\theta}$  gives

$$e^{i\theta} - \frac{(1 + \rho)s}{R} + \frac{\rho s^2 e^{-i\theta}}{R^2} = \frac{D e^{-i\theta(\tau-1)}}{R^\tau}. \tag{B2}$$

The real and imaginary parts of this reduce respectively to

$$\cos^2 \theta (\tau - 1) = \frac{R^{2\tau}}{D^2} [(1 + \rho s^2 / R^2) \cos \theta - (1 + \rho)s / R]^2 \tag{B3}$$

$$\cos^2 \theta (\tau - 1) = 1 - \frac{R^{2\tau}}{D^2} [(1 - \rho s^2 / R^2)^2 \sin^2 \theta]. \tag{B4}$$

Eliminating  $\cos^2 \theta (\tau - 1)$  between Eqs. (B3) and (B4) and writing  $D^2 (= D^2(\theta))$  as the subject of the formula, produces

$$D^2(\theta) = R^{2\tau} \left[ 1 + \frac{\rho^2 s^4}{R^4} + \frac{(1 + \rho)^2 s^2}{R^2} + 2 \frac{\rho s^2}{R^2} \cos 2\theta - \frac{2(1 + \rho)s}{R} \left( 1 + \frac{\rho s^2}{R^2} \right) \cos \theta \right]. \tag{B5}$$

$D^2$  is strictly increasing on  $0 < \theta < \pi$  if  $dD^2/d\theta$  can be shown to be positive for all  $\theta$  on  $0 < \theta < \pi$ . The derivative is

$$\frac{dD^2}{d\theta} = R^{2\tau} \left[ -4 \frac{\rho s^2}{R^2} \sin 2\theta + \frac{2(1 + \rho)s}{R} \left( 1 + \frac{\rho s^2}{R^2} \right) \sin \theta \right]. \tag{B6}$$

For  $D^2$  to be monotonically increasing its derivative must not have any roots on  $0 < \theta < \pi$ . (If it is monotonically increasing, then additional unique roots on the unit circle cannot exist.) If there is a root, then the functions  $u(\theta)$  and  $v(\theta)$  intersect, where we define

$$u(\theta) = a \sin 2\theta, \quad v(\theta) = \sin \theta \tag{B7}$$

and

$$a = \frac{2\rho s}{R(1 + \rho)(1 + \rho s^2 / R^2)}. \tag{B8}$$

Note that  $a > 0$  since  $0 < s < 1$ ,  $0 < \rho < 1/s$ , and  $R > 0$ . An intersection occurs at the endpoints of the interval, but not necessarily between  $0$  and  $\pi$ . Figure 10 is a schematic of the two functions. For an intersection to occur  $a \sin 2\theta$  must increase faster than  $\sin \theta$  at  $\theta = 0$ . The function  $a \sin 2\theta$  is then larger than  $\sin \theta$  for a domain of  $\theta$ , but crosses  $\sin \theta$  as it returns to zero for  $\theta = \pi/2$ . The condition for an intersection to occur then becomes

$$\frac{du(\theta)}{d\theta} > \frac{dv(\theta)}{d\theta} \tag{B9}$$

at  $\theta = 0$ . We have that

$$\frac{du(0)}{d\theta} = \frac{4\rho s}{R(1 + \rho)(1 + \rho s^2 / R^2)} \tag{B10}$$

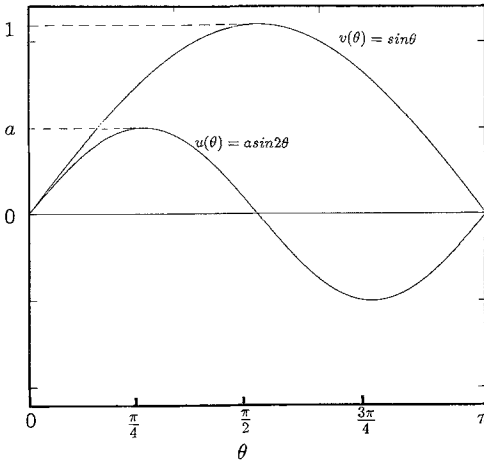


**Fig. 10.** Graphical representation of the functions  $u(\theta)$  ( $a \sin 2\theta$ ) and  $v(\theta)$  ( $\sin \theta$ ) (see Eq. (B7)) on the interval  $0 < \theta < \pi$ . For the case shown here, the functions do not intersect on  $0 < \theta < \pi$  and hence  $dD^2/d\theta$  is strictly positive

and

$$\frac{dv(0)}{d\theta} = 1. \tag{B11}$$

Intersection occurs if

$$\frac{4\rho s}{R(1+\rho)(1+\rho s^2/R^2)} > 1. \tag{B12}$$

An equivalent form of this condition for *no* intersection is

$$\frac{R}{\rho s} + \frac{R}{s} + \frac{s}{R} + \frac{\rho s}{R} \geq 4. \tag{B13}$$

The minimum of the left-hand side with respect to  $\rho$  is  $2 + R/s + s/R$  at  $\rho = R/S$ , and the minimum of  $2 + R/s + s/R$  is 4 (when  $R = s$ ).

Therefore the necessary condition that  $D^2$  is an increasing function of  $\theta$  for  $0 < \theta < \pi$  is satisfied for all  $0 < s < 1$ , all  $0 < \rho < 1/s$ , and all  $R > 0$ .

### Appendix C: Estimating the bias $\hat{D} - D$

The analysis by Walters and Ludwig (1981) assumes that the observation errors are such that any biomass estimate,  $\hat{B}_t$ , is lognormally distributed. The expected value of the estimate of  $B_t$  for any particular  $t$  is

$$E[B_t] = B_t e^{\sigma_v^2/2} \tag{C1}$$

where  $\sigma_v^2$  is the measurement variance in  $\ln \hat{B}_t$ . If the true values, the  $B_t$  themselves, are lognormally distributed with mean  $\bar{B}$ , where  $\bar{B} = 1/n \sum_{t=\tau}^{n-1+\tau} B_t$ , then the expected value of the estimated mean adult biomass values,  $\hat{\bar{B}}$  (where  $\hat{\bar{B}} = 1/n \sum_{t=\tau}^{n-1+\tau} \hat{B}_t$ ), over  $n$  years is given by

$$E[\hat{\bar{B}}] = \bar{B} e^{\sigma_v^2/(2n)} \tag{C2}$$

where  $\bar{B}$  is the true mean value and  $n$  are the number of years of data (note: the variance of the logarithm of the *mean* adult biomass estimate is  $\sigma_v^2/n$ ).

We consider the cases for which  $n > 10$  and  $\sigma_v < 0.5$  for which

$$1 < e^{\sigma_v^2/(2n)} < 1.0126 \tag{C3}$$

The value of  $\sigma_v$  of 0.50 corresponds to a coefficient of variation of biomass estimate around true value of 53% (the coefficient of variation of a lognormal variable is  $\sqrt{e^{\sigma^2} - 1}$ ,  $\sigma^2$  being the variance of the logarithm of the random variable). Therefore, from (C4), the difference between actual and observed mean adult biomass will be less than 1.26%. Similarly, the difference between  $\ln(\bar{R}/\bar{B})$  and  $\ln(\hat{R}/\hat{B})$  (where  $\ln(\hat{R}/\hat{B})$  is the mean value,  $1/n \sum_{t=\tau}^{n-1+\tau} \ln(\hat{R}_t/\hat{B}_{t-\tau})$ ) will be less than 1.26% if the recruitment estimate is lognormally distributed with a coefficient of variation of  $\sigma_v^2$ .

An acceptable regression procedure would therefore be to force the regression function to pass through the observed mean point,  $[\ln(\hat{R}/\hat{B}), \hat{B}]$ , which we argue will be very close to the true mean point,  $[\ln(\bar{R}/\bar{B}), \bar{B}]$ . From this it is possible to obtain an estimate of  $\alpha$ , if  $\hat{\beta}$ ,  $\ln(\hat{R}/\hat{B})$  and  $\hat{B}$  are given. If for convenience the time subscripts are ignored, the recruitment function (82) can be rewritten as

$$\ln(R/B) = \ln \alpha - \beta B. \quad (C4)$$

From the preceding discussion, it is reasonable to assume that

$$\hat{B} \approx \bar{B} \quad (C5)$$

and

$$\overline{\ln(\hat{R}/\hat{B})} \approx \overline{\ln R/B}. \quad (C6)$$

Thus, if the estimated stock-recruitment function passes through the estimated mean point, it also passes through the true mean point. Hence the true stock-recruitment function intersects with the estimated stock-recruitment function at the estimated mean point, so that the following relationship holds

$$\ln(\hat{\alpha}) - \hat{B}\hat{\beta} = \ln \alpha - \bar{B}\beta. \quad (C7)$$

Using approximation (C6), Eq. (C7) can be rearranged and exponentiated to obtain

$$\hat{\alpha} = \alpha e^{(\hat{\beta}-\beta)\bar{B}}. \quad (C8)$$

Substituting the equation for  $B^*$  ((85) main text) into the equation for  $D$  ((86) main text) gives

$$D = (1-s) \left( 1 - \ln \frac{\alpha}{1-s} \right). \quad (C9)$$

From Eq. (C1), if  $s$  is known, the estimate of the slope of the recruitment function at equilibrium is

$$\hat{D} = (1-s) \left( 1 - \ln \frac{\hat{\alpha}}{1-s} \right). \quad (C10)$$

Therefore, replacing  $\hat{\alpha}$  by  $\alpha e^{(\hat{\beta}-\beta)\bar{B}}$  in (C10),  $\hat{D}$  becomes

$$\hat{D} = (1-s) \left( 1 - \ln \frac{\alpha}{1-s} - (\hat{\beta}-\beta)\bar{B} \right). \quad (C11)$$

Subtracting the left- and right-hand sides of Eq. (C1) from the left- and right-hand sides of Eq. (C11), the bias in the estimate of the slope of the recruitment function at equilibrium is

$$\hat{D} - D = -(1-s)(\hat{\beta}-\beta)\bar{B}. \quad (C12)$$

## References

- Allen, K. R.: Analysis of stock-recruitment relations in Antarctic fin whales. Rapp. P.-v. Reun. Cons. int. Explor. Mer. **164**, 132-137 (1970)
- Beverton, R. J. H., Holt, S. J.: On the dynamics of exploited fish populations. Fish. Invest., ser. 2, **19**. London: Ministry of Agriculture (1957)
- Botsford, L. W., Wickam, D. E.: Behaviour of age-specific, density-dependent models and the northern Californian dungeness crab (*Cancer magister*) fishery. Can. J. Fish. Aquat. Sci. **35**, 833-843 (1978)
- Clark, W.: A delayed-recruitment model of population dynamics, with an application to baleen whale populations. J. Math. Biol. **3**, 381-391 (1976)
- Cushing, D. H.: Dependence of recruitment on parent stock. J. Fish. Res. Board Can. **30**, 1965-1976 (1973)

- Deriso, R. B.: Non-linear age-structured models for seasonally breeding populations. Ph.D. dissertation, Biomathematics program. Seattle: University of Washington (1978)
- Deriso, R. B.: Harvesting strategies and parameter estimation for an age-structured model. *Can. J. Fish. Aquat. Sci.* **37**, 268–282 (1980)
- Deriso, R. B., Hoag, S. H., McCaughran, D. A.: Two hypotheses about factors controlling production of Pacific halibut. *International North Pacific Fisheries Commission Bulletin Number 47*, 167–173 (1985)
- Fisher, M. E., Goh, B. S.: Stability results for delayed-recruitment models in population dynamics. *J. Math. Biol.* **19**, 147–156 (1984)
- Fowler, C. W., Smith, T. D.: Characterizing stable populations: an application in the African elephant population. *J. Wildl. Manage.* **37**, 513–523 (1973)
- Getz, W. M.: The ultimate sustainable yield problem in nonlinear age structured populations. *Math. Biosci.* **48**, 279–292 (1980)
- Getz, W. M.: Harvesting discrete nonlinear age and stage-structured populations. *J. Optimization Theory Appl.* **57**, 69–83 (1988)
- Getz, W. M., Haight, R.: *Population harvesting: Demography models of fish, forest, and animal resources*. Princeton: Princeton University (1989)
- Goh, B. S.: Stability in a stock-recruitment model of an exploited fishery. *Math. Biosci.* **33**, 359–372 (1977)
- Guckenheimer, J., Oster, G., Ipaktchi, A.: The dynamics of density dependent population models. *J. Math. Biol.* **4**, 101–147 (1977)
- Hightower, J. E., Grossman, G. D.: Comparison of constant effort harvesting policies for fish stocks with variable recruitment. *Can. J. Fish. Aquat. Sci.* **42**, 982–988 (1985)
- Leslie, P. H.: On the use of matrices in certain population mathematics. *Biometrika.* **35**, 183–212 (1945)
- Levin, S. A., May, R. M.: A note on difference-delay equations. *Theor. Popul. Biol.* **9**, 178–187 (1976)
- Levin, S. A., Goodyear, C. P.: Analysis of an age-structured fishery model. *J. Math. Biol.* **9**, 245–274 (1980)
- Marden, M.: *Geometry of polynomials*. Providence: American Mathematical Society 1966
- May, R. M.: Biological populations with non-overlapping generations: stable points, stable cycles and chaos. *Science.* **186**, 645–647 (1974)
- May, R. M.: Models for single populations. In: May, R. M. (ed.) *Theoretical ecology: principles and applications*, pp. 4–25. Oxford, London: Blackwell 1976
- May, R. M., Conway, G. R., Hassel, M. P., Southwood, T. R. E.: Time delays, density dependence, and single species oscillations. *J. Anim. Ecol.* **43**, 747–770 (1974)
- May, R. M., Oster, G. F.: Bifurcations and dynamic complexity in simple ecological models. *Am. Nat.* **110**, 573–599 (1976)
- Minc, H., Marcus, M.: *A survey of matrix theory and matrix inequalities*. Boston: Prindle, Weber and Schmidt 1964
- Reed, W. J.: Optimum age-specific harvesting in a nonlinear population model. *Biometrics* **36**, 579–593 (1980)
- Schaffer, W. M.: Stretching and folding in lynx fur returns: evidence for a strange attractor in nature? *Am. Nat.* **124**, 798–820 (1984)
- Schnute, J.: A general theory for analysis of catch and effort data. *Can. J. Fish. Aquat. Sci.* **42**, 414–429 (1985)
- Schnute, J., Fournier, D.: A new approach to length-frequency analysis: growth structure. *Can. J. Fish. Aquat. Sci.* **37**, 1337–1351 (1980)
- Shepherd, J. G.: A versatile new stock-recruitment relationship for fisheries, and the construction of sustainable yield curves. *J. Cons. int. Explor. Mer.* **40**(1), 67–75 (1982)
- Tuljapurkar, S.: Cycles in nonlinear age-structured models I. renewal equations. *Theor. Popul. Biol.* **32**, 26–41 (1987)
- Wachter, K. W.: Elusive cycles. Are there dynamically possible Lee-Easterlin models for U.S. births. Sloan-Berkeley Working Paper #2–3 (1987)
- Walters, C. J., Ludwig, D.: Effects of measurement errors on the assessment of stock-recruitment relationships. *Can. J. Fish. Aquat. Sci.* **38**, 704–710 (1981)